

# High repetition-rate LPP-source facility for EUVL

T. Schmid\*, S. A. George, J. Cunado, S. Teerawattanasook, R. Bernath,  
C. Brown, K. Takenoshita, C.-S. Koay, and M. Richardson

College of Optics & Photonics, 4000 Central Florida Blvd, Orlando, Florida, USA

## ABSTRACT

In this work we present the status of our high repetition-rate/high power EUV source facility. The mass-limited target concept has demonstrated high conversion efficiencies (CE) previously, with precision solid state lasers. Currently, experiments are in progress with high power high repetition-rate (3-4 kHz) Q-switched laser modules. We present a new dedicated facility for the high power EUV source. Also, we present a precision EUV energy-meter, which is developed for absolute EUV energy measurements. Spectral measurements of the tin-doped droplet laser plasma are performed with a flat-field spectrometer (FFS) with a back-illuminated CCD camera. We address the issue of maintaining the calibration of the EUV optics during source operation at non-optimum intensity at high repetition-rate, which is required for CE improvement studies. Here we present the unique metrology for measuring EUV energies under a variety of irradiation conditions without degrading EUV optics, even at high repetition rates (multi-kHz).

**Keywords:** EUVL, laser produced plasma, high power, high repetition-rate

## 1. INTRODUCTION

Providing EUV sources with sufficient source power and long lifetime is crucial for the introduction of EUVL<sup>1</sup>. Several hot dense plasma sources based on discharge plasmas and laser produced plasmas are being developed to meet the requirements for EUVL<sup>2</sup>, where the required source power of 115 W at the Intermediate Focus (IF), as well as the lifetime, the source etendue, and the spectral purity are specified. To provide high EUV power, efficient source plasmas are needed. The reflectivity of EUV optics, which can be reduced by debris from the source plasma, has to remain within a 10% reflectivity drop from its original value for the required lifetime.

We have previously reported on the important fundamental characteristics of the EUV source plasma, generated using tin-doped droplet targets<sup>3,4</sup>. Using a low repetition rate but well-characterized solid state laser (Nd:YAG), a high conversion efficiency (CE) of 2% was demonstrated, using the mass-limited<sup>5,6</sup> tin-doped droplet target approach<sup>3</sup>. The debris generated from the target is characterized in terms of tin aerosols and ion flux<sup>7,8,9</sup>. The tin aerosols would cause a reduction of the collector mirror lifetime. However, only a very limited number of generated tin aerosols are observed when the target is irradiated at the laser condition for high CE<sup>8</sup>. The plasmas generated with tin-doped droplets exhibit not only the high CE and the low debris, but also the small source size<sup>10</sup> and low out-of-band radiation<sup>11</sup>.

The collector mirror lifetime is expected to be shortened with source operation at increased repetition rates. We have conducted Monte-Carlo simulations to predict the mirror lifetime with the calculated surface erosion rates under the measured ion flux. The lifetime estimated for the typical Si/Mo multilayer (ML) mirror coating was approximately a factor of 500 shorter than the required lifetime<sup>12</sup>. However, the mirror lifetime can be extended by the use of debris mitigation schemes, which reduce the ion flux at the mirror

---

\*tschmid@creol.ucf.edu; phone 1 407 823-6855; fax 1 407 823-6880; www.creol.ucf.edu

surface. We have developed two types of electromagnetic field mitigation schemes which will ensure that the collector mirror reflectivity remains high for the entire lifetime<sup>12,13,14</sup>.

To operate the source plasma at high repetition rates, the target supply, as well as the laser operation, have to be coupled at high frequencies. The tin-doped droplet target already exhibits its high repetition rate operation (10-100 kHz), which provides the opportunity of using high repetition rate lasers. This enables the generation of EUV sources scalable to power levels required for EUVL by either a single laser module, or by multiple laser modules multiplexed. In the latter approach, commercially available high power lasers can be used to irradiate the target.

We describe here a new EUV test facility suitable to demonstrate the generation of high EUV power with high power lasers, which may be multiplexed spatially and temporally. It comprises a vacuum chamber capable of providing a low enough vacuum for a high repetition rate source plasma generation and ports to couple several laser modules onto the target. It is important to have the capability of measuring the EUV energy without having the EUV optics degraded. For absolute EUV energy measurements the EUV ML-mirrors have to be calibrated. Due to the high source repetition rate even a small amount of debris could cause mirror reflectivity degradation and a loss of calibration. Therefore, a metrology has been adapted, which allows accurate EUV energy measurements without losing the calibration of the EUV optics.

This paper describes a source facility developed for the next generation of high EUV powers. The tin-doped droplet target scheme is summarized in the next section. The vacuum chamber setup for the high power EUV generation, as well as the diagnostics, is described. Also, the metrology adapted for the high repetition rate EUV source is presented in this paper.

## 2. TIN-DOPED DROPLET TARGET TECHNOLOGY

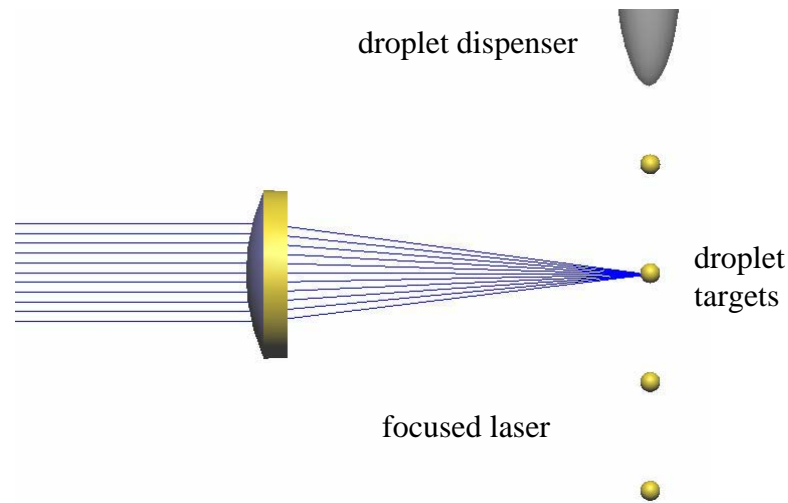


Fig.1. Droplet target stream with the laser beam focused on a droplet.

The tin-doped droplet target can be used as a mass-limited target<sup>3</sup>. The concept of a mass-limited target<sup>5,6</sup> is based on complete ionization of the target material. This is accomplished by reducing the size and consequently the mass of the target, so that only sufficient radiating species are included as required for an efficient high brightness EUV source. To operate the laser produced plasma source mass-limited, the focus size has to be adjusted relative to the target size to fully ionize the target. Consequently, only ions emitted from the plasma are a threat for impacting the collector mirror reflectivity.

To realize an ideal target for EUVL sources, tin atoms are doped into the water-based droplet with the minimum amount to produce EUV radiation. The droplet size is equivalent to the size of the laser focus, which was previously measured to be  $\sim 30 \mu\text{m}^3$ . A single droplet target contains about  $10^{13}$  tin atoms. The mass of tin would be too large if the same size of droplet would contain only tin atoms. Therefore, we have designed the target supply scheme with a capillary nozzle and a piezo-electric crystal, which produces a micro droplet stream producing spherical droplets of typically  $35\mu\text{m}$  diameter. The targets are supplied at a repetition rate of  $10 \sim 100 \text{ kHz}$ . With this target repetition rate, scaling up the EUV source power is possible to meet the source power requirements for EUVL.

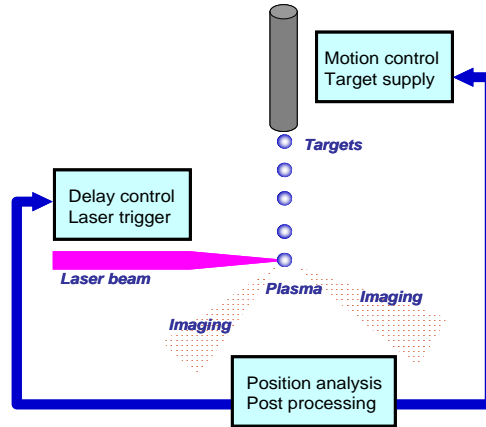


Fig.2. Principle of automatic feedback system

The CE has been shown to be a function of laser intensity<sup>3</sup>. Consequently, the laser intensity can be optimized by varying the focus position relative to the target position. It has been shown for tin-doped droplet targets experimentally, that the highest CE is obtained for intensities of  $\sim 10^{11} \text{ W/cm}^2$ <sup>3</sup>. As mentioned earlier, at the operating conditions for highest CE, the number of aerosols is minimized<sup>8</sup>. In contrast, the number of aerosols is much larger in the lower laser intensities<sup>8</sup>. The small number of tin aerosols observed during a long term plasma operation at the optimum intensity was caused by positioning the target manually with respect to the laser, and therefore slight displacement of the target from the focal spot lead to lower intensities.

To overcome the problem of precisely positioning the target continuously, an automatic targeting system has been developed. The system consists of a droplet position sensing scheme, data processing, and feedback for controlling the target and laser synchronization. Two visible imaging systems are integrated as the position sensing scheme. Back-illumination of the droplets, for imaging through the two axes, uniquely defines the position of the droplet. The images are fed to a computer which performs image processing techniques to determine the position. Once the computer receives images of the droplets, it computes the position of the droplet. If the software finds that the droplet position has changed, the droplet is physically moved back into position. Fig.2 illustrates the feedback system. This process runs continuously.

### 3. HIGH POWER EUV SOURCE FACILITY

#### 3.1 New Laser Plasma EUV Source Facility

We have assembled a new EUV source facility for high EUV power generation. A new vacuum chamber is installed and dedicated to high power EUV generation (Fig.3). A vacuum of  $< 10^{-4}$  torr is achieved with a combination of a high flow dry pump and a turbo-molecular pump. The chamber is equipped with a variety of ports, allowing several different diagnostics to be concurrently used as well as multiple beam

illumination of the target. The lasers are installed in a separate room, routed to the vacuum chamber, and are coupled into the chamber through AR-coated windows. The target can be illuminated from various angles. To adjust the spot size and consequently the intensity at the target position, the focusing lenses are mounted on motorized linear translation stages, which enable the adjustment of the lens positions during the experiment. By moving the lenses, the coupling conditions of the laser and the droplet can be optimized for highest CE. The current design of the source facility is kept flexible to incorporate future extensions, such as a collector mirror installation, debris mitigation systems and diagnostic instruments. Due to the configuration of the source chamber, the EUV source can be evaluated at the intermediate focus. For target delivery, a droplet dispenser is installed inside the source chamber. An advanced targeting system has been integrated, which was described above.

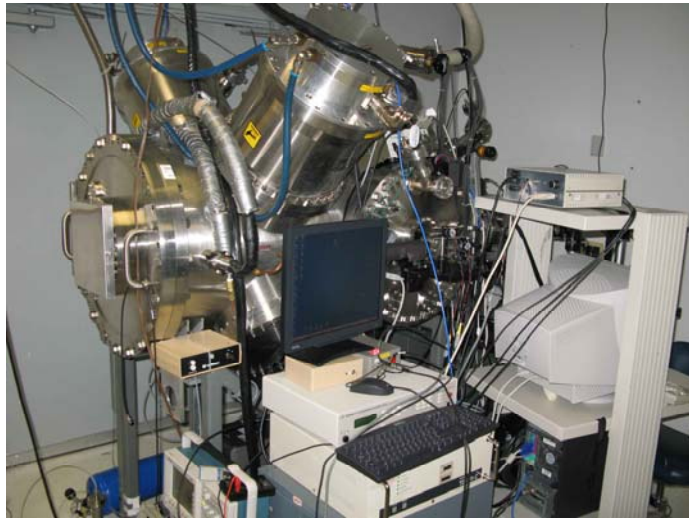


Fig.3. Vacuum chamber equipped with turbo pumps and diagnostics

### 3.2 EUV Diagnostics

In our experiments, several sets of calibrated spectroscopic and EUV metrological tools are used. As we scale tests to high repetition rates and higher EUV powers, the methodology and operation of these instruments will change. For our present tests a new energy-monitor was built for absolute EUV energy measurements. This is separate from the existing flying circus (FC) so as to provide for an adapted metrology for high repetition rate EUV source operation, described in the next section. The energy-monitor, shown in Fig.4, includes a 45 degree flat ML-mirror and a zirconium filter to eliminate out of band radiation, which were calibrated at NIST. The EUV signal is detected with a biased photodiode (AXUV-100)<sup>15</sup> connected to an oscilloscope. Prior to the installation to the new chamber the EUV monitor was also cross-calibrated with the FC<sup>16</sup> with EUV radiation generated on the tin-doped droplet plasmas at low repetition rate.

To optimize the plasma temperature for the highest CE, a grazing incidence flat-field spectrometer (FFS), shown in Fig.5, coupled with a back-illuminated X-ray CCD camera was deployed<sup>17,18</sup>. The FFS provides time-integrated, high-resolution spectra in the relevant wavelength region (12.5 nm – 18.5 nm). A laser control system was developed to control the exact number of pulses during one exposure time of the FFS. Therefore, the deposited energy into the plasma is known. To avoid artifacts in the spectrum caused by EUV photons during the readout time of the X-ray CCD, the number of pulses was limited to 128 when taking CE measurements. Fig.6 shows a typical spectrum taken from the tin-doped droplet laser plasma, where the CE was higher than 2.0%. The spectrometer was cross-calibrated to the energy-monitor and used in the CE optimization, described in more detail in the next section.

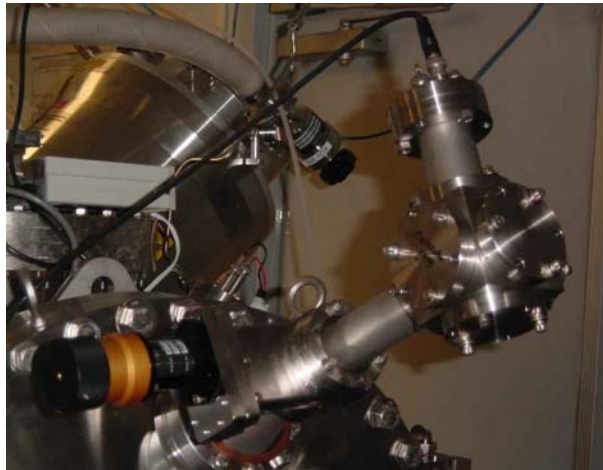


Fig.4. Calibrated EUV energy-meter

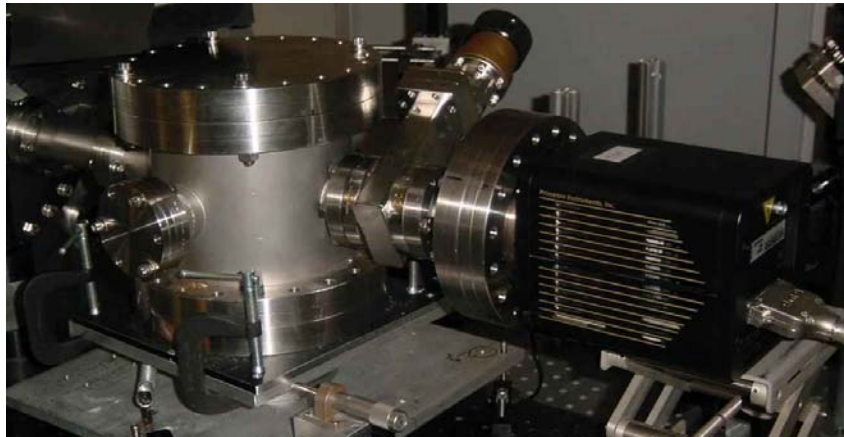


Fig.5. Flat-Field Spectrometer with Xray-CCD

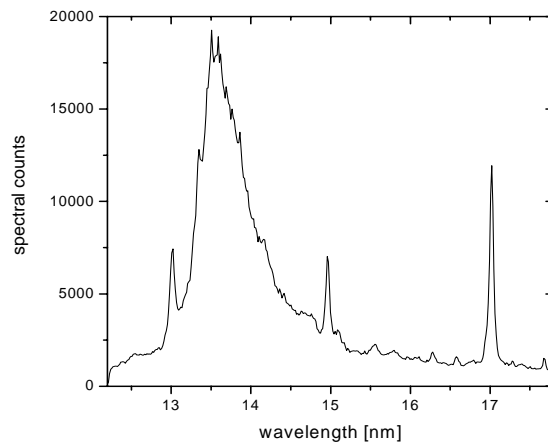


Fig.6. Typical spectrum (tin-doped droplet target) taken with the FFS

## 4. METROLOGY

### 4.1 Standard method for estimating CE

CE is an important parameter for laser produced plasma sources, determining how efficient laser energy is converted to EUV radiation. Before the adapted metrology for high repetition rate EUV source operation is described, it is useful to review the CE calculation process<sup>3,19</sup>. To determine the laser energy an energy-meter or power-meter is used. The in-band EUV energy is calculated by taking all wavelength dependent parameters of the components in the FC into account, together with a reference spectrum. The in-band EUV energy is calculated as<sup>3</sup>

$$E_{BW} = \frac{2\pi}{\Omega_s \cdot R_{scope}} \cdot \left[ \frac{\int_{BW} I_s(\lambda) d\lambda}{\int_{all} I_s(\lambda) T_{gas}(\lambda) R_{mirror}(\lambda) T_{filter}(\lambda) \eta_{diode}(\lambda) d\lambda} \right] A_{scope} \quad \text{Equ.1.}$$

where  $\Omega_s$  is the collection solid angle of the EUV detection,  $A_{scope}$  is the integrated area under the EUV signal waveform displayed on an oscilloscope,  $R_{scope}$  is the impedance of the oscilloscope channel,  $T_{gas}(\lambda)$  is the transmission function of the gas in the vacuum chamber,  $R_{mirror}(\lambda)$  is the calibrated mirror reflectivity curve,  $T_{filter}(\lambda)$  is the transmission curve of the filter(s) used to block visible light from entering the AXUV detector,  $\eta_{diode}(\lambda)$  is the calibrated responsivity curve of the AXUV detector in the FC,  $I_s(\lambda)$  is the spectrum of the EUV source. The constant  $\Omega_s$  is calculated with the mirror diameter for the FC and the source mirror distance, since the full aperture of the reflected EUV radiation will be detected by the photodiode. The filter transmission and the mirror reflectivity are calibrated at NIST and the characteristics are shown in Fig.7.

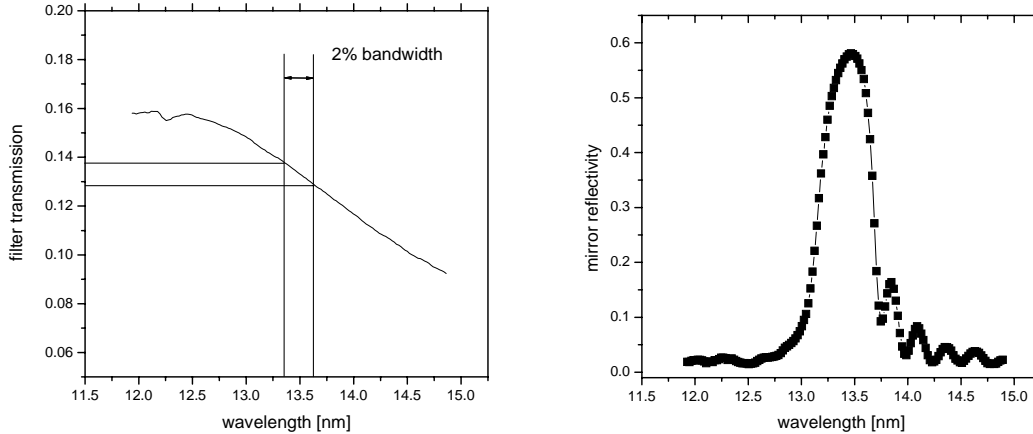


Fig.7. Transmission of zirconium filter (left); Multilayer reflectivity (right)

We have used a calibrated photodiode that measures a small reflection (4%) of the laser energy at a pellicle surface for the laser energy measurement. The laser energy and EUV energy are measured simultaneously to calculate the CE of a single EUV plasma generation<sup>3</sup>. Therefore the CE is calculated as

$$CE_i = \frac{E_{BW,i}}{E_{laser,i}} \cdot 100\% . \quad \text{Equ.2.}$$

## 4.2 Adaption of metrology for high repetition rate plasmas

Measuring EUV and laser energy at high repetition rates is more challenging than at a low repetition rate. Also, the CE optimization needs to be done while the plasmas generated can degrade the reflectivity of the ML-mirror. As described above, at lower than optimum intensities for highest CE, tin aerosols are generated. Thus, we have adapted a methodology for EUV energy measurements at high repetition rates while the EUV optics is not degraded.

The exposed area of the EUV mirror can be reduced to preserve the high reflectivity over a large number of plasma exposures. The energy-monitor, which is mounted on the new vacuum chamber for high power EUV source operation, utilizes a flat mirror with the highest reflectivity at an angle of incidence of 45 degree and the AXUV detector after the mirror. Only a fraction of the reflected EUV is detected by the detector. Therefore, in this configuration reducing the exposure area on the ML-mirror by installing a limiting aperture in front of the mirror is easily possible.

Despite the effort to reduce the exposure area on the mirror, the mirror will degrade eventually. We instead utilize the FFS as in-band EUV energy measurement instrument by cross-calibrating it against the energy-monitor, which is described next. With this method, CE optimization by changing the lens position with regard to the target position can be done without degrading any EUV optics. Thus, the EUV energy-monitor remains calibrated and is used only for the calibration process, which is done after the intensity has been optimized for high CE and low aerosol generation. A gate valve located between the plasma source and the energy-meter is only opened briefly for the calibration of the FFS to the energy-meter. Therefore the EUV mirror is only exposed for a very few shots during the calibration procedure.

The laser pulse energy can be measured for each laser pulse. However, averaging the laser energy as well as the EUV energy is a more reasonable approach for high repetition rate (~kHz) plasmas. The EUV energy measurements are based on the time integrated spectra. Similarly, measuring the laser power instead of measuring each laser pulse is preferable. For the CE measurement an average laser energy is used, which is calculated from the measured power of the laser and the repetition rate of the laser.

## 4.3 Cross-calibration of energy-monitor and FFS

To avoid reflectivity degradation of the ML-mirror of the energy-monitor, a FFS is installed at the high power source chamber to measure the EUV energy based on the spectrum. Because of the small collimating slit (120 $\mu$ m) and a source-slit distance of 585mm, negligible effects on the calibration are expected. Here, the cross-calibration process and the EUV energy measurement based on the FFS spectrum are described.

Introducing the constant  $K_S$  and the bandwidth coefficient  $BW_{coeff}$  the in-band energy, Equ. 1 can be expressed

$$E_{BW} = K_S \cdot A_{scope} \cdot BW_{coeff} \quad \text{Equ.3.}$$

with

$$K_S = \frac{2\pi}{\Omega_S \cdot R_{scope} \cdot \eta_{diode}} \quad \text{Equ.4.}$$

where  $\eta_{diode}$  is assumed to be constant, and

$$BW_{coeff} = \frac{\int_{BW} I_S(\lambda) d\lambda}{\int_{all} I_S(\lambda) T_{gas}(\lambda) R_{mirror}(\lambda) T_{filter}(\lambda) d\lambda}. \quad \text{Equ.5.}$$

The product of  $K_s$  and  $A_{scope}$  is the EUV energy emitted from the plasma into  $2\pi$  sr, based on the energy measured by the photodiode.  $BW_{coeff}$  represents the ratio of the EUV energy inside 2% spectral band at 13.5 nm to the total energy measured by the photodiode.

Because  $A_{scope}$  is a result of the radiation reflected and transmitted through the components

$$A_{scope} \propto \int_{all} I_S(\lambda) T_{gas}(\lambda) R_{mirror}(\lambda) T_{filter}(\lambda) d\lambda . \quad \text{Equ.6.}$$

By introducing a calibration coefficient  $K_{spec}$  for the FFS spectrometer, based on a given number of shots, slit size and the distance, the measured EUV energy can be calculated as

$$K_s \cdot A_{scope} = K_{spec} \int_{all} I_S(\lambda) T_{gas}(\lambda) R_{mirror}(\lambda) T_{filter}(\lambda) d\lambda \quad \text{Equ.7.}$$

where the coefficient  $K_{spec}$  has units of J(into  $2\pi$ )/(spectral counts). By substituting Equ. 7 into Equ. 3, the in-band EUV energy can be written as

$$E_{BW} = K_{spec} \cdot \int_{BW} I_S(\lambda) d\lambda . \quad \text{Equ.8.}$$

This means the spectral counts inside the bandwidth are converted to in-band energy (into into  $2\pi$  sr solid angle, within 2% bandwidth, centered on 13.5 nm). Therefore, the cross-calibration of FFS in-band spectral counts to the in-band energy calculated based on Equ.1<sup>3,16</sup> is established.

For an arbitrary spectral measurement,

$$E_{BW,i} = K_{spec} \cdot \int_{BW} I_{S,i}(\lambda) d\lambda \quad \text{Equ.9.}$$

where  $E_{BW,i}$  is the in-band energy into  $2\pi$  sr and  $I_{S,i}$  is the spectral intensity of the particular measurement. Therefore, only FFS measurements are needed to obtain the in-band EUV energies for the CE optimization.

## 5. CONCLUSION

We report the status of our installations regarding a high power EUV source facility. The facility includes droplet generation at high repetition rates, high power laser systems and EUV diagnostic instruments. The diagnostic instruments were calibrated to the flying circus II instrument, to allow for calibrated energy measurements. To maintain the calibration of the diagnostics, a procedure was presented to calibrate spectral measurements from a FFS with an absolutely calibrated EUV energy-meter. The calibrated FFS allows source operation at non-optimum intensities at high repetition-rate for CE optimization studies. The facility, the diagnostic instruments, and the cross-calibration method will be adopted for source operations at even higher repetition rates for the future extension.

## ACKNOWLEDGEMENTS

The authors acknowledge useful discussions with Dr. William Silfvast and the technical support of: Dr. Greg Shimkaveg, and Somsak Terrawattanasook. This work is supported by funds from SRC, Powerlase LTD, (UK) and the State of Florida.



## REFERENCES

1. V.Y. Banine, J.P.H. Benschop, H.G.C. Werij, "Comparison of Extreme Ultraviolet Sources for Lithography Applications," *Microelectronic Eng.* 53, pp.681-684, (2000).
2. K. Ota, Y. Watanabe, H. Franken, and V. Banine, "EUV Source Requirements," 2004 EUV Source Workshop (Miyazaki, Japan, November 2004).
3. C-S. Koay, S. George, K. Takenoshita, "High conversion efficiency microscopic tin-doped droplet target laser- plasma source for EUVL," *Proc. SPIE* 5751, pp. 279-292 (2005).
4. M. C. Richardson, C.-S. Koay, K. Takenoshita, C. Keyser, "High conversion efficiency mass-limited Sn-based laser plasma source for EUV lithography," *Journal of Vacuum Science and Technology B*, volume 22, number 2, pages 785-790, March 2004.
5. F. Jin, K. Gabel, M. C. Richardson, M. Kado, A. F. Vassiliev, D. Salzmann, "Mass-limited laser plasma cryogenic target for 13-nm point x-ray sources for lithography," *Proc. SPIE*, vol. 2015, pp. 151-159, 1993
6. C. Keyser, C.-S. Koay, K. Takenoshita, M. C. Richardson, I.C.E. Turcu, "High conversion efficiency mass-limited laser plasma source for EUV lithography," *Proceedings of CLEO*, June 2003.
7. K. Takenoshita, C.-S. Koay, S. Teerawattanasook, M. C. Richardson, "Debris studies for the tin-based droplet laser-plasma EUV source," *Proceedings of SPIE, Emerging Lithographic Technologies VIII*, volume 5374, pages 954-963, 2004.
8. K. Takenoshita, C.-S. Koay, S. Teerawattanasook, M. C. Richardson, "Debris characterization and mitigation from microscopic laser-plasma tin-doped droplet EUV sources," *Proceedings of SPIE*, volume 5751, 2005.
9. K. Takenoshita, C.-S. Koay, S. A. George, S. Teerawattanasook, M. C. Richardson, V. Bakshi, "Ion emission measurements and mirror erosion studies for extreme ultraviolet lithography," *Journal of Vacuum Science and Technology B*, volume 23, number 6, pages 2879-2884, 2005.
10. C.-S. Koay, "Radiation Studies of the tin-doped microscopic droplet laser plasma light source specific to EUV Lithography," Ph. D. thesis, University of Central Florida, 2006.
11. S. George, K. Takenoshita, R. Bernath, T. Schmid, C.-S. Koay, M. Al-Rabban, M.C. Richardson "XUV spectroscopy of mass-limited Sn-doped laser micro-plasmas," *SPIE Advanced Lithography* 2007
12. K. Takenoshita, "Debris characterization and mitigation of droplet laser plasma sources for EUV lithography," Ph. D. thesis, University of Central Florida, 2006.
13. K. Takenoshita, C.-S. Koay, M. C. Richardson, I.C.E. Turcu, "The repeller field debris mitigation approach for EUV sources," *Emerging Lithographic Technologies VII*, SPIE, volume 5037, pages 792-800, 2003.
14. T. Schmid, K. Takenoshita, C.-S. Koay, S. George, S. Teerawattansook, M. Richardson, "Debris mitigation for high-NA laser plasma EUV sources," *SPIE Microlithography* 2006.
15. International Radiation Detection (California, USA).
16. S.A. van der Westen, C. Bruineman, F. Bijkerk, and V. Bakshi, "Flying Circus 2: Calibration of an Extreme Ultraviolet Source at PLEX LLC," *International SEMATECH Technology Transfer #04024490A-TR* (2004), available at <http://www.sematech.org>.
17. X-ray CCD camera model: PI-SX:512 from Princeton Instrument.
18. W. Schwanda, K. Eidmann, and M. C. Richardson, "Characterization of a flat-field grazing-incidence XUV spectrometer," *J. X-ray Sci. and Tech.*, vol. 4, pp. 8-17 (1993).
19. C-S. Koay, K. Takenoshita, E. Fujiwara, M. Al-Rabban, M. Richardson, "Spectroscopic studies of the Sn-based laser plasma EUV source," *Proc. SPIE* 5374, pp. 964-970 (2004).